NIH Public Access
Author Manuscript
ACS Chem Biol. Author manuscript; available in PMC 2010 March 20.

Published in final edited form as:
ACS Chem Biol. 2009 March 20; 4(3): 209–220. doi:10.1021/cb800304d.

The Molecular Basis of Species-Specific Ligand Activation of Trace Amine-Associated Receptor 1 ($TAAR_1$)

Edwin S. Tan[a,e], **John C. Naylor**[d], **Eli S. Groban**[b], **James R. Bunzow**[d], **Matthew P. Jacobson**[c], **David K. Grandy**[d], and **Thomas S. Scanlan**[c,d,f]

a*Chemistry and Chemical Biology Graduate Program, University of California, San Francisco, San Francisco, CA 94158-2280*

b*Graduate Group in Biophysics, University of California, San Francisco, San Francisco CA 94158-2240*

c*Department of Pharmaceutical Chemistry, University of California, San Francisco, San Francisco, CA 94158, USA*

d*Department of Physiology and Pharmacology, Oregon Health and Science University, Portland, OR 97239, USA*

Abstract

The trace amine-associated receptor **1** ($TAAR_1$) is an aminergic G protein-coupled receptor (GPCR) potently activated by 3-iodothyronamine (**1**), an endogenous derivative of thyroid hormone. Structure activity relationship studies on **1** and related agonists showed that the rat and mouse species of $TAAR_1$ accommodated structural modifications and functional groups on the ethylamine portion and the biaryl ether moiety of the molecule. However, the two receptors clearly exhibited distinct, species-specific ligand preferences despite being remarkably similar with 93% sequence similarity. In this study, we generated single and double mutants of rat and mouse $TAAR_1$ to probe the molecular recognition of agonists and the underlying basis for the ligand selectivity of rat and mouse $TAAR_1$. Key, non-conserved specificity determinant residues in transmembranes helices 4 and 7 within the ligand binding site appear to be the primary source of a number of the observed ligand preferences. Residue 7.39 in transmembrane 7 dictated the preference for a β-phenyl ring while residue 4.56 in transmembrane 4 was partially responsible for the lower potency of **1** and **tyramine** for the mouse receptor. Additionally, **1** and **tyramine** were found to have the same binding mode in rat $TAAR_1$ despite structure activity relationship data suggesting the possibility of each molecule having different binding orientations. These findings provide valuable insights into the critical binding site residues involved in the ligand-receptor interaction that can influence compound selectivity and functional activity of aminergic GPCRs.

INTRODUCTION

3-Iodothyronamine (**1**, T_1AM; Fig. 1) is an endogenous derivative of the thyroid hormone thyroxine (T_4; Fig. 1) detected in the brain, heart, liver, and blood (1,2). It has profound pharmacological effects *in vivo* that are mostly opposite to those of T_4 (3). Compound **1** induces anergia, hypothermia, bradycardia, hyperglycemia, and hyperinsulinemia when administered to mice and rapidly reduces cardiac output in an *ex vivo* working rat heart preparation (2,4–

fCorrespondence should be addressed to T.S.S. (E-mail: scanlant@ohsu.edu; phone (503) 494-9292; fax (503) 494-9275).
ePresent Address: Department of Systems Biology, Harvard Medical School, 200 Longwood Avenue, WA 536, Boston, MA 02115, USA

Supporting Information Available: This material is available free of charge via the Internet.

NIH-PA Author Manuscript
NIH-PA Author Manuscript
NIH-PA Author Manuscript

NIH-PA Author Manuscript

NIH-PA Author Manuscript

NIH-PA Author Manuscript

8). Additionally, **1** can increase food intake and influence energy metabolism by favoring lipid utilization over carbohydrate consumption (9,10).

These physiological responses to **1** may be mediated by more than one molecular target. *In vitro*, **1** can activate aminergic G protein-protein coupled receptors (GPCRs) in the biogenic amine subfamily; stimulating the production of cAMP (adenosine 3′,5′-cyclic monophosphate) via the trace amine-associated receptor 1 ($TAAR_1$) and the degradation of cAMP via the α_{2A} adrenergic receptor (2,7,11,12). Additionally, **1** has a neuromodulatory role, inhibiting neurotransmitter reuptake by the dopamine (DAT) and norepinephrine transporter (NET), and inhibiting vesicular packaging by the vesicular monoamine transporter 2 (VMAT2) (13).

To date, **1** is the most potent endogenous molecule that can activate rat and mouse $TAAR_1$. $TAAR_1$ is a member of the trace amine-associated receptor family of orphan GPCRs, which consists of 19 rat, 16 mouse, and 9 human subtypes (14–18). It is homologous to the dopamine, adrenergic, and serotonin receptors and expressed in multiple tissues including the heart, kidney, liver, spleen, and pancreas. Although a biological function for any TAAR subtype has yet to be defined, rodent and human species of $TAAR_1$ are potently activated by endogenous biogenic amines such as β-phenethylamine as well as the psychostimulants amphetamine and methamphetamine in a species-dependent manner (12,14,15,19–21). In addition, other members of the rodent TAAR family were recently implicated as a secondary class of chemosensory receptors expressed in the olfactory epithelium (22).

In an effort to determine the role of $TAAR_1$ in mediating the effects of **1**, we have previously explored the structure activity relationship (SAR) of **1** and developed a number of analogs with improved agonist activity (11,23). These SAR studies showed rat and mouse $TAAR_1$ ($rTAAR_1$ and $mTAAR_1$, respectively) could tolerate structural modifications and substituents on the ethylamine portion and biaryl ether moiety of **1**. However the two receptors clearly have distinct structural preferences. In the ethylamine chain, for example, $rTAAR_1$ favored unsaturated hydrocarbon substituents while $mTAAR_1$ preferred polar groups and hydrogen bond acceptors (23). Compound **1** and **tyramine** (Table 1), an endogenous phenethylamine metabolite, also exhibited some degree of species variability, being ~7 to 10-fold less potent for $mTAAR_1$ compared to $rTAAR_1$ (11). These distinct ligand selectivities of rat and mouse $TAAR_1$ are unusual given that the two receptors are 93% similar in primary sequence. Since the rodent receptors are only 83%–85% similar to human $TAAR_1$, understanding the molecular basis of species variability will undoubtedly have important implications in the development of activators and inhibitors for human $TAAR_1$. In this study, we explored the molecular recognition of **1** and related agonists by $TAAR_1$ and identified specificity determining residues that give rise to the disparate ligand preferences between rat and mouse $TAAR_1$.

RESULTS AND DISCUSSION

Our initial structure activity relationship study identified the β-phenylphenoxy-phenethylamine (**2** & **3**) and phenoxynaphethylamine (**4**) as promising scaffolds for the development of small molecule regulators of $TAAR_1$ (Fig. 1) (23). Compounds **2** and **3** were both $rTAAR_1$ selective, being 357- to 526-fold more potent for $rTAAR_1$ compared to $mTAAR_1$ (Table 1). Compound **4**, on the other hand, was less discriminating between rat and mouse $TAAR_1$ with a disparity in potency of 5-fold between the two receptors. Using the toggle switch model of aminergic GPCR activation as a guideline, **2** was further developed to give superagonists (agonists that are more potent and/or efficacious than **1**) **5**, **6**, and **7** (Table 1) (24). These superagonists remained $rTAAR_1$ selective exhibiting potencies that were ≥ 1600- to 2500-fold better at $rTAAR_1$ versus $mTAAR_1$.

NIH-PA Author Manuscript

NIH-PA Author Manuscript

NIH-PA Author Manuscript

The poor agonist activity of the β-phenylphenoxyphenethylamines at $mTAAR_1$ can be attributed to the β-phenyl group of the molecule and not its outer ring moiety (Fig. 1). Removing the outer rings of **2** and **5** (**8** and **9**, respectively) did not increase potency at $mTAAR_1$ (Table 1). Both **8** and **9** still activated $mTAAR_1$ poorly with a potency ≥10μM. In contrast, eliminating the β-phenyl ring of **2**, **5**, and **7** to give **1** or **10** improved the potency at $mTAAR_1$ ~24- to 32-fold and decreased the $rTAAR_1$ selectivity from ≥ 350- to 2500-fold down to ~7–10-fold.

Aminergic GPCRs are heptahelical transmembrane proteins with an extracellular amino terminus and an intracellular carboxy terminus (Fig. 2a). The ligand binding site of aminergic GPCRs is located within the transmembrane (TM) region of the receptor and is predominantly composed of residues from TM 3, 5, 6 and 7 (25–28). Based on pharmacological and mutagenesis studies, epinephrine is proposed to bind to the β_2-adrenergic receptor (β_2AR) with aspartic acid 3.32 (D3.32) acting as the counterion for the charged amine, serine residues 5.42, 5.43, and 5.46 (S5.42, S5.43, and S5.46, respectively) interacting with the catechol hydroxyls, phenylalanines 6.51 and 6.52 (F6.51 and F6.52) interacting with the catechol ring, and asparagines 6.55 (N6.55) as the partner for the β-hydroxy group (Fig. 2b) (see experimental procedures for a description of the residue indexing system) (29–36). In the recently solved crystal structure of an engineered human β_2AR, all of these residues were found to line the ligand binding site and interact with the inverse agonist that co-crystallized with the receptor (26,27). By analogy to the catecholamine receptors (dopamine, epinephrine, and norepinephrine) we have previously deduced **2** to bind to $rTAAR_1$ with the charged amine forming a salt bridge interaction with D3.32 and the biaryl ether oxygen hydrogen bonding to S5.46 (Fig. 2c) (24). In this binding orientation, our homology model of $rTAAR_1$ showed the β-phenyl ring to be positioned near the interface between TM 6 and 7 and surrounded by cysteine 6.54, methionine 6.55, and asparagines 7.35 and 7.39 (C6.54, M6.55, N7.35, and N7.39, respectively).

In $mTAAR_1$, C6.54 and N7.35 are conserved but not M6.55 and N7.39. Instead $mTAAR_1$ has a threonine and tyrosine at 6.55 and 7.39, respectively (T6.55 and Y7.39) (Fig. 2d). In the β_2AR, the residues at 6.55 and 7.39 have been previously shown to interact with the ligand and alter the receptor's ligand specificity (35,37). Since the β-phenyl ring is proposed to be in the vicinity of 6.55 and 7.39, and both residues are not conserved between rat and mouse $TAAR_1$, we hypothesized that one or both of these residues are specificity elements that influence compatibility with the β-phenyl ring of the β-phenylphenoxyphenethylamine scaffold. We tested this hypothesis by measuring the activity of **3** and **5**, representative β-phenylphenoxyphenethylamines, against rat and mouse $TAAR_1$ in HEK293 (human embryonic kidney 293) cells stably and heterologously expressing single or double swap mutants at 6.55 and/or 7.39.

Residue 7.39 controls specificity for the β-phenyl ring of $TAAR_1$ ligands

Swapping residue 6.55 of rat and mouse $TAAR_1$ had minor effects on the activity and selectivity of **3** and **5**. In the $rTAAR_1$ 6.55 single mutant [$rTAAR_1$(M6.55T)] the potency and efficacy of **3** (EC_{50} = 55 ± 20 nM, E_{max} = 119 ± 6%) and **5** (EC_{50} = 11 ± 1 nM, E_{max} = 117 ± 20%) decreased 2- to 3-fold and ≤ 12%, respectively (Table 2). When T6.55 was mutated to a methionine in $mTAAR_1$ [$mTAAR_1$(T6.55M)], both compounds were still poor agonists activating the receptor with potencies >10μM and efficacies ranging from 20% to 45%. Despite the mutation at residue 6.55, both **3** and **5** remained considerably $rTAAR_1$ selective (182- to 909-fold) (Fig. 3).

The single swap mutants at residue 7.39 had opposing effects on the activity of **3** and **5**. The potency of both compounds decreased 167- to 526-fold in the $rTAAR_1$ 7.39 mutant [$rTAAR_1$(N7.39Y)] (EC_{50} = ~10 μM and ~1 μM for **3** and **5**, respectively) but increased 60- to 100-fold in its $mTAAR_1$ 7.39 mutant counterpart [$mTAAR_1$(Y7.39N)] (EC_{50} = 102 ± 21

NIH-PA Author Manuscript

NIH-PA Author Manuscript

NIH-PA Author Manuscript

nM and 176 ± 32 nM for **3** and **5**, respectively) (Table 2). The efficacy of **3** (E_{max} = 95 ± 6%) and **5** (E_{max} = 91 ± 11%) both increased 29% to 89% in $mTAAR_1$(Y7.39N). For $rTAAR_1$(N7.39Y) the efficacy of **5** (E_{max} = 126%) increased 12% while that of **3** (E_{max} = 85%) decreased 46% compared to wild type. Interestingly, swapping the residues at 7.39 converted both compounds to good $mTAAR_1$ agonists that were now 6- to 98-fold selective for $mTAAR_1$ over $rTAAR_1$ (Fig. 3).

The activity profile of **3** and **5** for the double swap mutants was similar to that of the 7.39 single mutants but showed some enhancements in both potency and efficacy. The potency of **3** and **5** decreased 333- to 526-fold for the $rTAAR_1$ 6.55 and 7.39 double mutant [$rTAAR_1$(M6.55T/N7.39Y)] but increased 70- to 320-fold for the $mTAAR_1$ 6.55 and 7.39 double mutant equivalent [$mTAAR_1$(T6.55M/Y7.39N)] (Table 2). The same trend was also observed with regards to efficacy; decreasing 44% to 85% for $rTAAR_1$(M6.55T/N7.39Y) and increasing 39% to 95% for $mTAAR_1$(T6.55M/Y7.39N). Compared to the 7.39 single mutant, the $mTAAR_1$ selectivity of **3** and **5** in the double mutant was more pronounced (Fig. 3).

The decrease in activity of **3** and **5** for the 6.55 and/or 7.39 single and double mutants in $rTAAR_1$ cannot be attributed to the introduced mutations compromising the functional competency of the receptors because the activity of the positive controls (**1** and **4**) for the same mutants only changed ≤ 4-fold and ≤ 16% in terms of potency and efficacy, respectively (Table 2). Likewise, the enhanced activity of **3** and **5** for the $mTAAR_1$ single and double swap mutants is not a consequence of the mutations rendering the receptors constitutively active and more responsive to agonists because the potency of the positive controls (**1**, **4**, and/or 11) only changed ≤ 2-fold and the efficacy were essentially identical compared to the wild type receptor (Table 1 and 2). Compound **11** is a novel agonist for rat and mouse $TAAR_1$ that can be considered a halogen free analog of **1**.

Swapping residues at 7.39 was sufficient to convert **3** and **5** from a $rTAAR_1$ into a $mTAAR_1$ selective agonist. The $TAAR_1$ binding site appears to be able to accommodate a phenyl ring in the interface between TM 6 and 7 within the binding site near residue 7.39. Compounds **3** and **5** are poor agonists for wild type $mTAAR_1$ because this phenyl pocket near 7.39 is occupied by the phenol group of Y7.39 from the receptor and unavailable to the β-phenyl rings of **3** and **5**. In contrast, **3** and **5** are excellent agonists for wild type $rTAAR_1$ because the smaller asparagine residue at 7.39 is less sterically encumbering and does not compete with the β-phenyl rings of **3** and **5** for the phenyl pocket near 7.39 of the receptor.

It should be noted that the substitution pattern of the outer ring does not significantly affect the specificity of $TAAR_1$ for β-phenyl ring bearing compounds. Regardless of whether the outer ring is at the *meta*- (**3**) or *para*- (**5**) position relative to the ethylamine chain, both **3** and **5** were affected similarly by mutations at 6.55 and/or 7.39 in rat and mouse $TAAR_1$, indicating that the β-phenyl ring of both molecules occupy the same binding pocket within the binding site. This result supports the assumptions we had proposed regarding the location of the antagonistic groups of the lead $rTAAR_1$ antagonists previously developed with **3** as the core scaffold (24).

Based on its primary sequence, we predict human $TAAR_1$ ($hTAAR_1$) to be able to accommodate a phenyl ring at the β carbon of phenethylamine based ligands because the residue at 7.39 in the human receptor is an isoleucine (Fig. 2e). Since isoleucine is smaller than tyrosine and approximately the same size as asparagine, the phenyl pocket near 7.39 should also be present in $hTAAR_1$.

Compound 1 and Tyramine have similar binding modes

In addition to being a superagonist for $rTAAR_1$, **7** (EC_{50} = 4 ± 1 nM, E_{max} = 115 ± 2%) is also an interesting molecule because it contains the structures of both **tyramine** (EC_{50} = 65 ± 1

NIH-PA Author Manuscript

NIH-PA Author Manuscript

NIH-PA Author Manuscript

nM, E_{max} = 119 ± 7%) and **1** (EC_{50} = 33 ± 3 nM, E_{max} = 100 ± 0%) in the same compound (Table 1 and Fig. 4). This hybrid compound potentially explains how two molecules with very different molecular volumes can elicit similar responses. If the β-phenyl group of **7** represents the aromatic ring of **tyramine**, then **tyramine** would occupy the phenyl pocket near 7.39 and thus have a binding mode different from **1** (Fig. 4). On the other hand, if the inner ring of **7** represents the **tyramine** aromatic ring then **tyramine** and **1** would have similar binding modes. The $rTAAR_1$ agonist activity of **9** (EC_{50} = 115 ± 12 nM, E_{max} = 105 ± 5%) supports the feasibility of **tyramine** potentially having two alternate binding modes in the rat receptor (Table 1). Since the tyrosine residue at 7.39 in $mTAAR_1$ abolished the phenyl pocket near 7.39, **tyramine** must share the same binding mode as **1** in $mTAAR_1$.

To determine if **tyramine** and **1** have similar or distinct binding modes, we mutated alanine 5.42 in $rTAAR_1$ to a threonine, leucine, or isoleucine [$rTAAR_1$(A5.42T), $rTAAR_1$(A5.42L), and $rTAAR_1$(A5.42I), respectively] and examined the effects of the mutations on the potency of **tyramine** and **1**. The idea behind these 5.42 single mutants is to perturb the pocket occupied by the outer ring of **1**, **7** and other biaryl ether containing molecules by introducing larger residues than alanine. Threonine was chosen because SAR studies on human $TAAR_1$, which has a threonine at residue 5.42 (Fig. 2e), showed **1** to be a less potent agonist against $hTAAR_1$ than $rTAAR_1$ (12).

In the $rTAAR_1$(A5.42L) mutant, the potency of **1** (EC_{50} = 58 ± 16 nM) and **tyramine** (EC_{50} = ~2 μM) decreased 2- and 31- fold, respectively (Table 3a). When A5.42 was mutated to isoleucine, there was a 3- and 154-fold decrease in the potency of **1** (EC_{50} = 108 ± 14 nM) and **tyramine** (EC_{50} = >10 μM), respectively. The efficacy of **tyramine** in the leucine mutant decreased 53% to 70% compared to wild type $rTAAR_1$. A similar trend was observed for the $rTAAR_1$(A5.42T) mutant where **1** (EC_{50} = 88 ± 13 nM) and **tyramine** (EC_{50} = >10 μM) were 3- and 154-fold less potent. Additionally, **tyramine** was 50% less efficacious for this receptor than wild type. Since the activity of the positive control (**11**) for all 5.42 mutants were essentially unaffected, the reduced activities of **1** and **tyramine** for these mutants cannot be due to a compromised activation capacity of these receptors.

The observed effects on the activity of **1** and **tyramine** in the $rTAAR_1$ 5.42 mutants are consistent with both compounds having similar binding modes. If **tyramine** preferentially occupied the phenyl pocket near residue 7.39, its potency would not have been affected by changes to residue 5.42. Since its activity decreased 31- to 154-fold when residue 5.42 was mutated, **tyramine** is probably binding to $rTAAR_1$ with its hydroxyl group engaged in hydrogen bond interactions with S5.46, the residue one turn below 5.42 in TM5 (Fig. 2d). This binding mode corresponds to the same binding orientation of **1** for rat and mouse $TAAR_1$.

Although the leucine and isoleucine mutations increased the steric bulk around residue 5.42, it is interesting that the agonist activity of the smaller **tyramine** was more severely affected than the larger **1** or **11**; especially when these mutations were intended to block the binding pocket for the outer ring. These results suggest that despite being bigger than alanine, leucine and isoleucine are not large enough to completely abolish the outer ring binding pocket or are sufficiently flexible to accommodate the outer phenyl ring. The small effects of the mutations on the agonist activity of **1** and **11** can potentially be attributed to their larger number of interactions with the receptor compared to **tyramine**. Like **tyramine**, **1** and **11** should both be anchored in the binding site of $rTAAR_1$ by a salt bridge interaction between the charged amine and D3.32, and a hydrogen bond interaction with S5.46. However, the extra functional groups present in **1** and **11** (i.e. outer ring, iodine, and naphthyl ring) (Table 1) can make additional interactions with TM 5 and 6 that are not available to **tyramine**. With more contacts to the receptor, **1** and **11** would be less sensitive to structural changes at residue 5.42 than **tyramine**.

NIH-PA Author Manuscript

NIH-PA Author Manuscript

NIH-PA Author Manuscript

Residue 4.56 is partially responsible for the lower potency of 1 for $mTAAR_1$

Within the thyronamine series, rat and mouse $TAAR_1$ had the same rank order potency but the potency values of individual compounds for the two receptors were not identical. In general, thyronamines are ~10-fold less potent for $mTAAR_1$ compared to $rTAAR_1$ (2,11). Assuming all ligands target the same binding pocket and lead to the same active receptor conformation, a possible explanation for this potency disparity can be attributed to a lower G-protein coupling efficiency for $mTAAR_1$ versus $rTAAR_1$. If this were the case, then it would be impossible to have an equipotent agonist for both receptors because $mTAAR_1$ would be inherently less sensitive to ligand activation than $rTAAR_1$. Since **12** was found to be an equipotent agonist for $rTAAR_1$ (EC_{50} = 65 ± 6 nM, E_{max} = 115 ± 2%) and $mTAAR_1$ (EC_{50} = 82 ± 17 nM, E_{max} = 112 ± 3%), the G-protein coupling efficiency of $mTAAR_1$ is comparable to that of $rTAAR_1$ (Table 1).

We hypothesized that the potency disparity of thyronamines was brought about by nonconserved amino acid(s) at key specificity determinant residues within the binding site. In particular, we speculated that tyrosine 4.56 (Y4.56) was primarily responsible for the ~10-fold lower potency of **1** for $mTAAR_1$. This residue was identified through a process of elimination based on the following five points: (1) since the binding sites for most aminergic GPCRs are located within the transmembrane regions of the receptor, all intracellular and extracellular loops as well as the amino- and carboxy-terminus were eliminated (28); (2) amino acid differences in TM 1 and 2 were eliminated because the binding site is primarily composed to TM 3, 4, 5, 6, and 7 (30); (3) since the ethylamine chain of **1** and **12** are exactly the same, non-conserved residues in TM 3, 6 and 7 cannot be responsible; (4) TM5 was eliminated because it is absolutely conserved between the two species; (5) the intracellular half of TM 4 was eliminated because the binding site of GPCRs is located in the extracellular half of the transmembrane region (Fig. 5). The only non-conserved residue remaining was Y4.56. In our homology models of rat and mouse $TAAR_1$, residue 4.56 was found to be in the vicinity of the purported outer ring binding pocket and could conceivably make contacts with the bound ligand. To test the importance of residue 4.56, we generated rat and mouse $TAAR_1$ single swap mutants at this location.

When Y4.56 of $mTAAR_1$ was converted to phenylalanine [$mTAAR_1$(Y4.56F)], the potency of **1** increased 5-fold from 314 ± 43 nM to 67 ± 17 nM (Table 1 and **3b**). Interestingly, the potency of **1** (EC_{50} = 38 ± 11 nM) for the tyrosine mutant of $rTAAR_1$ [$rTAAR_1$(F4.56Y)] was comparable to wild type $rTAAR_1$ (33 ± 3 nM). The same trend was also observed for **tyramine**; where its potency increased 7-fold in $mTAAR_1$(Y4.56F) (EC_{50} = 40 ± 13 nM) but remained unaffected in $rTAAR_1$(F4.56Y) (EC_{50} = 54 ± 11 nM). Since the agonist activity of the positive controls (**4** and **11**) for the mutants was comparable to that of the wild type receptors for both species, the mutations did not compromise the functional capacity of either receptors.

Residue 4.56 appears to play an important role in the lower potency of **1** for $mTAAR_1$. Swapping this residue with the corresponding residue found in $rTAAR_1$ increased the potency of **1** in $mTAAR_1$ to within two-fold of the potency value for wild type $rTAAR_1$. Interestingly, the potency of **tyramine** for $mTAAR_1$(Y4.56F) was equivalent to that of wild type $rTAAR_1$. Although mutating residue 4.56 improved the potency in the $mTAAR_1$ mutants, the reciprocal effect of **1** and **tyramine** becoming less potent for $rTAAR_1$(F4.56Y) was not observed. This indicates that 4.56 is only partially responsible and not the sole basis for the observed potency disparity of **1** and **tyramine** between the rat and mouse $TAAR_1$. Overall, these results implicate residue 4.56 in TM4 to affect ligand interaction and receptor activation.

NIH-PA Author Manuscript

NIH-PA Author Manuscript

NIH-PA Author Manuscript

CONCLUSION AND SIGNIFICANCE

The disparate ligand structural preferences exhibited by rat and mouse $TAAR_1$ can be attributed to key, non-conserved specificity determining residues within the binding site. Residue 7.39 appears to dictate the specificity for a β-phenyl ring; the results suggest that the bulky tyrosine residue at 7.39 in $mTAAR_1$ sterically clashed with the β-phenyl ring whereas the smaller asparagine at the same location in $rTAAR_1$ was more compatible and able to accommodate a β-phenyl moiety. The lower potency of **1** in $mTAAR_1$ was partly caused by the presence of a tyrosine at residue 4.56 rather than a phenylalanine. Although compound **7** implied the possibility of **1** and **tyramine** having different binding modes in the binding site of $rTAAR_1$, **1** and **tyramine** appear to have the same binding orientation.

With the recent developments and accomplishments in structure determination of the β_2 adrenergic receptor, the practicality of a structure-based drug design approach towards developing activators and inhibitors for aminergic GPCRs has never been so promising. A critical aspect to the success of this strategy will depend on having insights into the molecular basis of ligand recognition, the mechanism of GPCR activation, and the relationship of how these ligand-receptor interactions are relayed and translated into receptor activation or inhibition. The information presented herein should prove beneficial towards this cause as it provides valuable information regarding the binding site residues involved in ligand-receptor interactions that can influence compound specificity and functional activity of an aminergic GPCR.

METHODS

Residue Indexing Scheme

Residues are labeled relative to the most conserved amino acid in the transmembrane segment in which it is located (38). Asparagine 7.39, for example, is located in transmembrane 7 and precedes the most conserved residue by 11 positions. Proline 6.50 is the most conserved residue in TM6. This system simplifies the identification of corresponding residues in different GPCRs.

$TAAR_1$ Site-Directed Mutagenesis

$TAAR_1$ mutants were generated by using the QuikChange Site-Directed Mutagenesis Kit (Stratagene, La Jolla, CA). Primers were designed that coded for the desired mutation flanked with 10–15 base pairs of sequence. Complementary oligonucleotides were then used in PCR using an expression plasmid containing the desired receptor as template. The PCR product was digested with Dpn I and transformed into XL1 Blue competent cells. Colonies were picked and the DNA isolated was sequenced to confirm the mutation.

The DNA for the mutants was then used to transfect HEK293 cells using Fugene (Roche, Indianapolis, IN) and stable cell lines were made for further assays under G418 selection.

Homology Model of rat and mouse $TAAR_1$

The homology model for $rTAAR_1$ was created using the Prime software package (Schrödinger Inc.). The model was based on a sequence alignment of $rTAAR_1$ with the sequence of human β_2AR, for which a crystal structure was recently solved (Protein Data Bank accession code 2RH1), created using the “align GPCR” module (26,27). The modeling procedure involves side chain rotamer optimization and closure of chain breaks due to gaps in the sequence alignment using a previously published loop building and optimization algorithm (39). After building the complete model, additional side chain rotamer optimization, followed by backbone and side chain energy minimization, was performed on all non-conserved residues. The homology modeling program relies on the OPLS all atom force field (40–42) and a Generalized

NIH-PA Author Manuscript

NIH-PA Author Manuscript

NIH-PA Author Manuscript

Born solvent model (43,44) to evaluate the energy of different conformations and select the lowest energy structure as the final model.

Synthesis

Detailed synthetic procedures and characterization information for novel compounds **8**, **9**, **11**, and **12** are described in the supporting information.

In Vitro cAMP Agonist Activity Assay

Compounds were tested using the Hithunter cAMP XS kit (DiscoveRx) as described previously (24). Data were reported relative to **1** and expressed as $\%T_1AM$. The activity of **1** at 10μM was set as 100 $\%T_1AM$. Concentration-response curves were plotted and EC_{50} values were calculated with Prism software (GraphPad, San Diego, CA). Standard error of the mean was calculated from the EC_{50} and E_{max} values of each independent triplicate experiment by use of Prism Software.

Supplementary Material

Refer to Web version on PubMed Central for supplementary material.

Acknowledgements

This work was supported by grants from the National Institutes of Health (Grant DK52798 to T.S.S.), the Portland Methamphetamine Abuse Research Center (D.K.G), the OHSU President's Fund (D.K.G.), the Alfred P. Sloan Foundation (research fellowship to M.P.J.), and Ikaria, Inc. (T.S.S.). M.P.J. is a member of the Scientific Advisory Board of Schrödinger, Incorporated. The authors would also like to acknowledge thoughtful discussions with Dr. Edmund A. Reese.

References

1. Piehl S, Heberer T, Balizs G, Scanlan TS, Smits R, Koksch B, Kohrle J. Thyronamines are isozyme-specific substrates of deiodinases. Endocrinology 2008;149:3037–45. [PubMed: 18339710]
2. Scanlan T, Suchland K, Hart M, Chiellini G, Huang Y, Kruzich P, Frascarelli S, Crossley D, Bunzow J, Ronca-Testoni S, Lin E, Hatton D, Zucchi R, Grandy D. 3-Iodothyronamine is an endogenous and rapid-acting derivative of thyroid hormone. Nat Med 2004;10:638–642. [PubMed: 15146179]
3. Scanlan TS. 3-Iodothyronamine (T1AM): A new player on the thyroid endocrine team? . Endocrinology. 2008 Dec 30;[Epub ahead of print]
4. Chiellini G, Frascarelli S, Ghelardoni S, Carnicelli V, Tobias S, DeBarber A, Brogioni S, Ronca-Testoni S, Cerbai E, Grandy D, Scanlan T, Zucchi R. Cardiac effects of 3-iodothyronamine: a new aminergic system modulating cardiac function. FASEB J 2007;21:1597–1608. [PubMed: 17284482]
5. Doyle K, Suchland K, Ciesielski T, Lessov N, Grandy D, Scanlan T, Stenzel-Poore M. Novel thyroxine derivatives, thyronamine and 3-iodothyronamine, induce transient hypothermia and marked neuroprotection against stroke injury. Stroke 2007;38:2569–2576. [PubMed: 17690312]
6. Frascarelli S, Ghelardoni S, Chiellini G, Vargiu R, Ronca-Testoni S, Scanlan TS, Grandy DK, Zucchi R. Cardiac effects of trace amines: pharmacological characterization of trace amine-associated receptors. Eur J Pharmacol 2008;587:231–6. [PubMed: 18486124]
7. Regard JB, Kataoka H, Cano DA, Camerer E, Yin L, Zheng YW, Scanlan TS, Hebrok M, Coughlin SR. Probing cell type-specific functions of Gi in vivo identifies GPCR regulators of insulin secretion. J Clin Invest 2007;117:4034–43. [PubMed: 17992256]
8. Zucchi R, Ghelardoni S, Chiellini G. Cardiac effects of thyronamines. Heart Fail Rev. 2008 Nov 19; [Epub ahead of print]
9. Braulke LJ, Klingenspor M, DeBarber A, Tobias SC, Grandy DK, Scanlan TS, Heldmaier G. 3-Iodothyronamine: a novel hormone controlling the balance between glucose and lipid utilisation. Journal of Comparative Physiology B 2008;178:167–77.

NIH-PA Author Manuscript NIH-PA Author Manuscript NIH-PA Author Manuscript

10. Dhillo WS, Bewick GA, White NE, Gardiner JV, Thompson EL, Bataveljic A, Murphy KG, Roy D, Patel NA, Scutt JN, Armstrong A, Ghatei MA, Bloom SR. The thyroid hormone derivative 3-iodothyronamine increases food intake in rodents. Diabetes Obes Metab. 2008 Jul 29;[Epub ahead of print]
11. Hart M, Suchland K, Miyakawa M, Bunzow J, Grandy D, Scanlan T. Trace amine-associated receptor agonists: Synthesis and evaluation of thyronamines and related analogues. J Med Chem 2006;49:1101–1112. [PubMed: 16451074]
12. Wainscott D, Little S, Yin T, Tu Y, Rocco V, He J, Nelson D. Pharmacologic characterization of the cloned human trace amine-associated receptor1 (TAAR1) and evidence for species differences with the rat TAAR1. J Pharmacol Exp Ther 2007;320:475–485. [PubMed: 17038507]
13. Snead A, Santos M, Seal R, Miyakawa M, Edwards R, Scanlan T. Thyronamines inhibit plasma membrane and vesicular monoamine transport. ACS Chem Biol 2007;2:390–398. [PubMed: 17530732]
14. Borowsky B, Adham N, Jones K, Raddatz R, Artymyshyn R, Ogozalek K, Durkin M, Lakhlani P, Bonini J, Pathirana S, Boyle N, Pu X, Kouranova E, Lichtblau H, Ochoa F, Branchek T, Gerald C. Trace amines: Identification of a family of mammalian G protein-coupled receptors. Proc Natl Acad Sci U S A 2001;98:8966–8971. [PubMed: 11459929]
15. Bunzow J, Sonders M, Arttamangkul S, Harrison L, Zhang G, Quigley D, Darland T, Suchland K, Pasumamula S, Kennedy J, Olson S, Magenis R, Amara S, Grandy D. Amphetamine, 3,4-methylenedioxymethamphetamine, lysergic acid diethylamide, and metabolites of the catecholamine neurotransmitters are agonists of a rat trace amine receptor. Mol Pharmacol 2001;60:1181–1188. [PubMed: 11723224]
16. Lindemann L, Ebeling M, Kratochwil N, Bunzow J, Grandy D, Hoener M. Trace amine-associated receptors form structurally and functionally distinct subfamilies of novel G protein-coupled receptors. Genomics 2005;85:372–385. [PubMed: 15718104]
17. Gloriam DE, Bjarnadottir TK, Schioth HB, Fredriksson R. High species variation within the repertoire of trace amine receptors. Ann N Y Acad Sci 2005;1040:323–7. [PubMed: 15891052]
18. Gloriam DE, Bjarnadottir TK, Yan YL, Postlethwait JH, Schioth HB, Fredriksson R. The repertoire of trace amine G-protein-coupled receptors: large expansion in zebrafish. Mol Phylogenet Evol 2005;35:470–82. [PubMed: 15804416]
19. Grandy D. Trace amine-associated receptor 1-Family archetype or iconoclast? Pharmacology and Therapeutics 2007;116:355–90. [PubMed: 17888514]
20. Reese E, Bunzow J, Arttamangkul S, Sonders M, Grandy D. Trace amine-associated receptor 1 displays species-dependent stereoselectivity for isomers of methamphetamine, amphetamine, and para-hydroxyamphetamine. J Pharmacol Exp Ther 2007;321:178–186. [PubMed: 17218486]
21. Zucchi R, Chiellini G, Scanlan T, Grandy D. Trace amine-associated receptors and their ligands. Br J Pharmacol 2006;149:967–978. [PubMed: 17088868]
22. Liberles S, Buck L. A second class of chemosensory receptors in the olfactory epithelium. Nature 2006;442:645–650. [PubMed: 16878137]
23. Tan E, Miyakawa M, Bunzow J, Grandy D, Scanlan T. Exploring the structure-activity relationship of the ethylamine portion of 3-iodothyronamine for rat and mouse trace amine-associated receptor 1. J Med Chem 2007;50:2787–2798. [PubMed: 17497842]
24. Tan ES, Groban ES, Jacobson MP, Scanlan TS. Toward deciphering the code to aminergic G protein-coupled receptor drug design. Chem Biol 2008;15:343–53. [PubMed: 18420141]
25. Bridges TM, Lindsley CW. G-protein-coupled receptors: from classical modes of modulation to allosteric mechanisms. ACS Chem Biol 2008;3:530–41. [PubMed: 18652471]
26. Cherezov V, Rosenbaum DM, Hanson MA, Rasmussen SG, Thian FS, Kobilka TS, Choi HJ, Kuhn P, Weis WI, Kobilka BK, Stevens RC. High-resolution crystal structure of an engineered human beta2-adrenergic G protein-coupled receptor. Science 2007;318:1258–65. [PubMed: 17962520]
27. Rosenbaum DM, Cherezov V, Hanson MA, Rasmussen SG, Thian FS, Kobilka TS, Choi HJ, Yao XJ, Weis WI, Stevens RC, Kobilka BK. GPCR engineering yields high-resolution structural insights into beta2-adrenergic receptor function. Science 2007;318:1266–73. [PubMed: 17962519]
28. Tota MR, Candelore MR, Dixon RA, Strader CD. Biophysical and genetic analysis of the ligand-binding site of the beta-adrenoceptor. Trends Pharmacol Sci 1991;12:4–6. [PubMed: 1848734]

NIH-PA Author Manuscript

NIH-PA Author Manuscript

NIH-PA Author Manuscript

29. Liapakis G, Ballesteros J, Papachristou S, Chan W, Chen X, Javitch J. The forgotten serine - A critical role for Ser-203(5.42) in ligand binding to and activation of the beta(2)-adrenergic receptor. J Biol Chem 2000;275:37779–37788. [PubMed: 10964911]
30. Shi L, Javitch J. The binding site of aminergic G protein-coupled receptors: The transmembrane segments and second extracellular loop. Annu Rev Pharmacol Toxicol 2002;42:437–467. [PubMed: 11807179]
31. Strader C, Candelore M, Hill W, Dixon R, Sigal I. A single amino-acid substitution in the beta-adrenergic-receptor promotes partial agonist activity from antagonists. J Biol Chem 1989;264:16470–16477. [PubMed: 2570781]
32. Strader C, Candelore M, Hill W, Sigal I, Dixon R. Identification of 2 serine residues involved in agonist activation of the beta-adrenergic-receptor. J Biol Chem 1989;264:13572–13578. [PubMed: 2547766]
33. Strader C, Fong T, Tota M, Underwood D, Dixon R. Structure and function of G-protein-couple receptors. Annu Rev Biochem 1994;63:101–132. [PubMed: 7979235]
34. Strader C, Sigal I, Candelore M, Rands E, Hill W, Dixon R. Conserved aspartic-acid residue-79 and residue-113 of the beta-adrenergic-receptor have different roles in receptor function. J Biol Chem 1988;263:10267–10271. [PubMed: 2899076]
35. Wieland K, Zuurmond H, Krasel C, Ijzerman A, Lohse M. Involvement of Asn-293 in stereospecific agonist recognition and in activation of the beta(2)-adrenergic receptor. Proc Natl Acad Sci U S A 1996;93:9276–9281. [PubMed: 8799191]
36. Zuurmond H, Hessling J, Bluml K, Lohse M, Ijzerman A. Study of interaction between agonists and Asn293 in helix VI of human beta(2)-adrenergic receptor. Mol Pharmacol 1999;56:909–916. [PubMed: 10531394]
37. Suryanarayana S, Daunt D, Von Zastrow M, Kobilka B. A point mutation in the 7th hydrophobic domain of the alpha-2 adrenergic-receptor increases its affinity for a family of beta-receptor-antagonists. J Biol Chem 1991;266:15488–15492. [PubMed: 1678390]
38. Ballesteros J, Weinstein H. Integrated methods for the construction of three-dimensional models of structure-function relations in G protein-coupled receptors. Methods Neuroscience 1995;25:366–428.
39. Jacobson MP, Pincus DL, Rapp CS, Day TJ, Honig B, Shaw DE, Friesner RA. A hierarchical approach to all-atom protein loop prediction. Proteins 2004;55:351–67. [PubMed: 15048827]
40. Jacobson M, Kaminski G, Friesner R, Rapp C. Force field validation using protein side chain prediction. J Phys Chem B 2002;106:11673–11680.
41. Jorgensen W, Maxwell D, Tirado-Rives J. Development and testing of the OPLS all-atom force field on conformational energetics and properties of organic liquids. J Am Chem Soc 1996;118:11225–11236.
42. Kaminski G, Friesner R, Tirado-Rives J, Jorgensen W. Evaluation and reparametrization of the OPLS-AA force field for proteins via comparison with accurate quantum chemical calculations on peptides. J Phys Chem B 2001;105:6474–6487.
43. Gallicchio E, Zhang LY, Levy RM. The SGB/NP hydration free energy model based on the surface generalized born solvent reaction field and novel nonpolar hydration free energy estimators. J Comput Chem 2002;23:517–29. [PubMed: 11948578]
44. Ghosh A, Rapp C, Friesner R. Generalized born model based on a surface integral formulation. J Phys Chem B 1998;112:10983–10990.

NIH-PA Author Manuscript

NIH-PA Author Manuscript

NIH-PA Author Manuscript

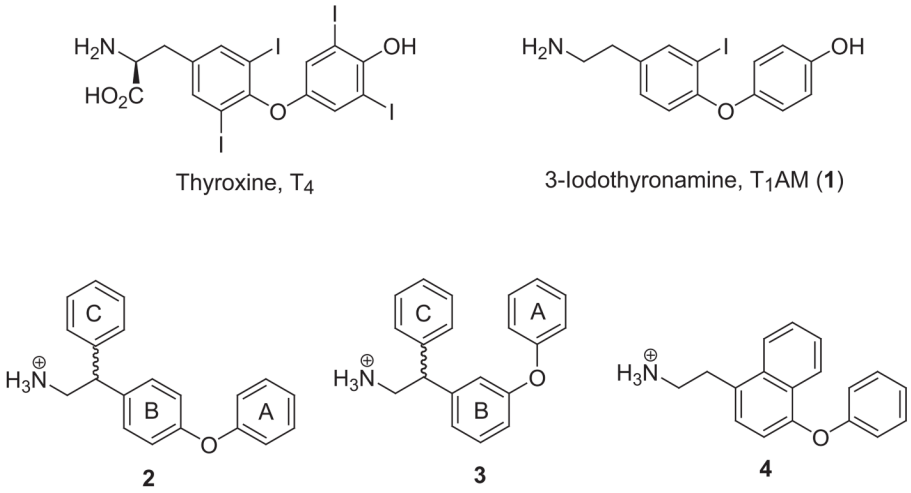

Figure 1.

Thyroid hormone, 3-iodothyronamine, and related analogs. Structures of thyroxine, 3-iodothyronamine (**1**), β-phenylphenoxyphenethylamines (**2** and **3**), and phenoxynaphethylamine (**4**). The A, B, and C rings of **2** and **3** correspond to the outer, inner, and β-phenyl rings, respectively.

NIH-PA Author Manuscript

NIH-PA Author Manuscript

NIH-PA Author Manuscript

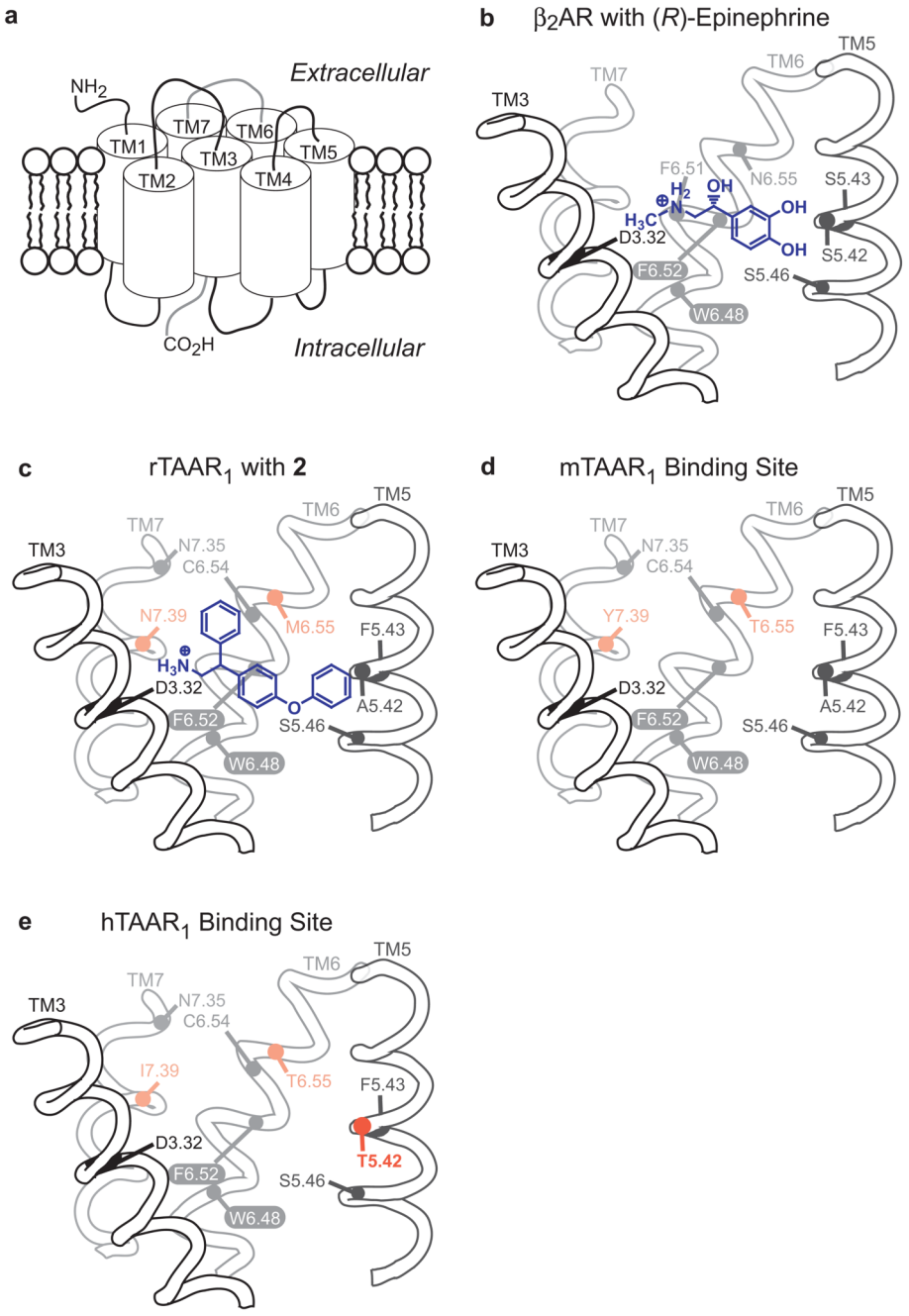

Figure 2.

Biogenic amine GPCRs. (**a**) Schematic representation of the helical arrangement of GPCRs viewed from the cell membrane. (**b**) Binding orientation of (*R*)-epinephrine in the binding site of the β_2AR. (**c**) Proposed binding orientation of **2** in the binding site of rTAAR$_1$. (**d**) Binding site of mTAAR$_1$. (**e**) Binding site of hTAAR$_1$. The binding sites of β_2AR, rTAAR$_1$, and mTAAR$_1$ are viewed from the perspective TM4. The rotamer switch residues (white letters), proposed binding and specificity determinant residues are labeled. Non-conserved residues that were mutated are shown in red.

NIH-PA Author Manuscript

NIH-PA Author Manuscript

NIH-PA Author Manuscript

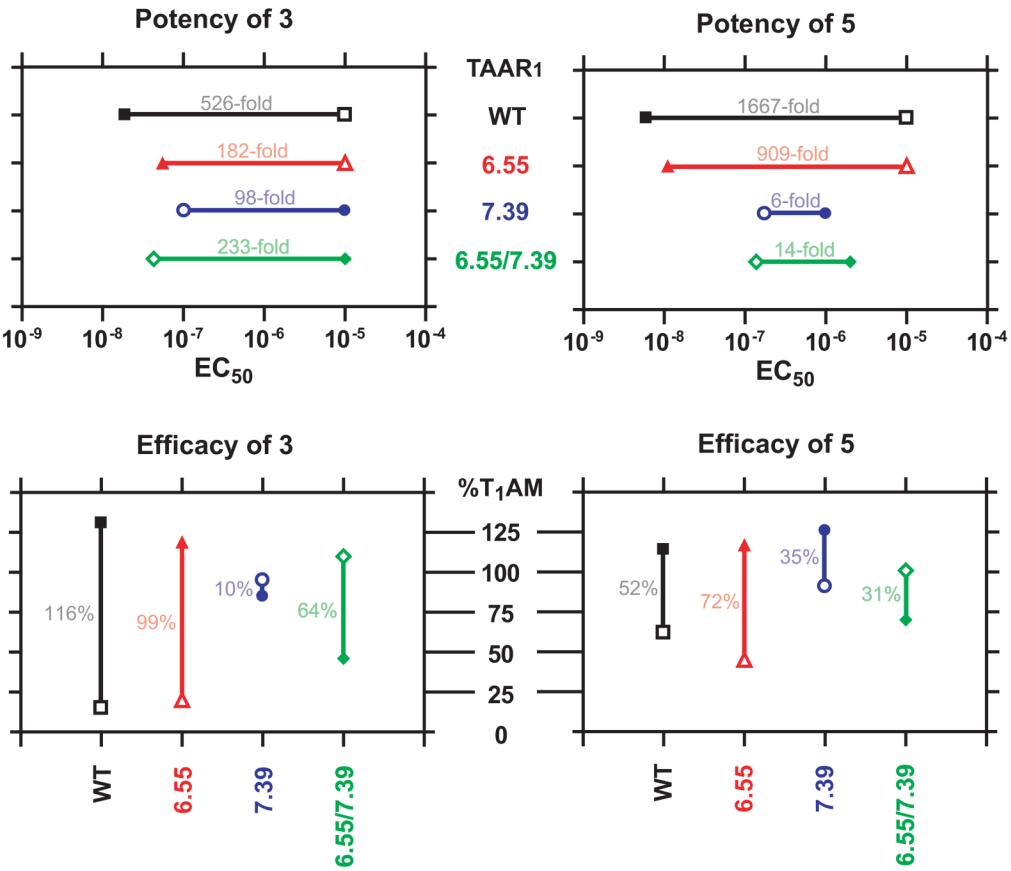

Figure 3.

Selectivity profiles of **3** and **5** on rat and mouse $TAAR_1$ wild type and mutant receptors. The top and bottom panels show the potency and efficacy, respectively, of **3** and **5**. The EC_{50} and E_{max} for $rTAAR_1$ and $mTAAR_1$ receptors are depicted in solid and hollow symbols, respectively. WT $rTAAR_1$ [■], $rTAAR_1$(M6.55T) [▲], $rTAAR_1$(N7.39Y) [●], $rTAAR_1$(M6.55T/N7.39Y) [♦], WT $mTAAR_1$ [□], $mTAAR_1$(T6.55M) [△], $mTAAR_1$(Y7.39N) [○], and $mTAAR_1$(T6.55M/Y7.39N) [◊]. The lines connecting the solid and hollow symbols represent the difference in potency (top panels) and efficacy (bottom panels) between rat and mouse TAAR1 receptors. The fold difference in potency and percent difference in efficacy are listed above (top panels) and to the left (bottom panels) of the connecting lines, respectively.

NIH-PA Author Manuscript

NIH-PA Author Manuscript

NIH-PA Author Manuscript

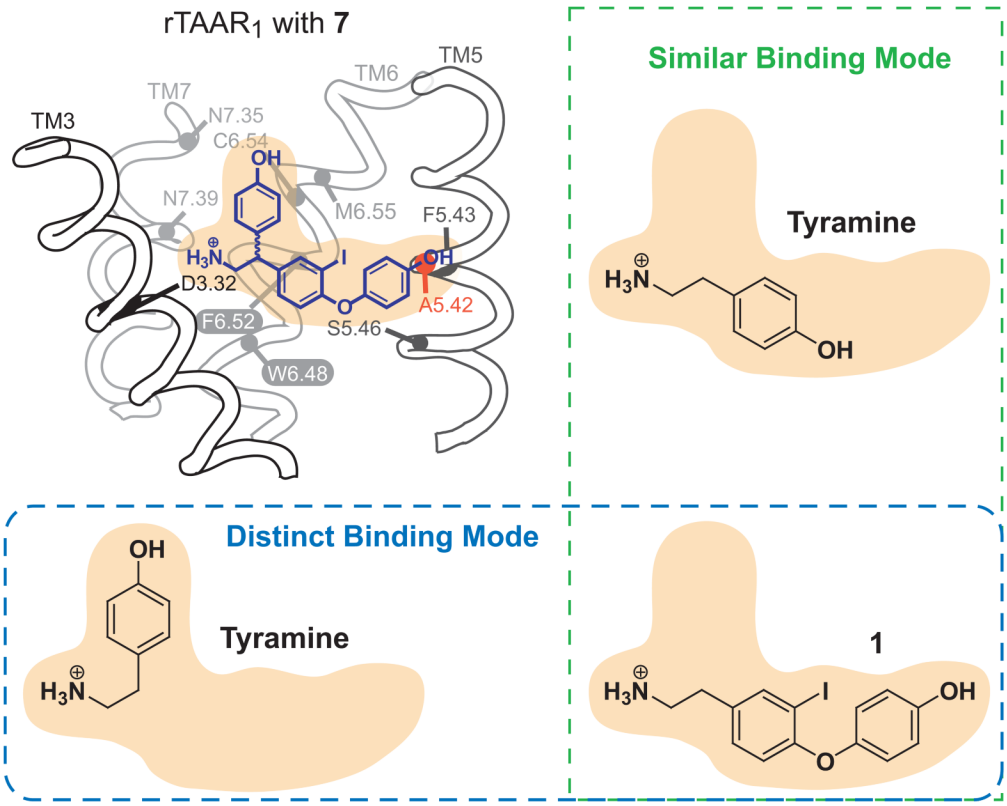

Figure 4.

Proposed binding modes of **7**, **1**, and **tyramine** in $rTAAR_1$. The binding site of $rTAAR_1$ is viewed from the perspective of TM4 (see Fig. 2a). The rotamer switch residues (white letters), proposed binding and specificity determinant residues are labeled. Residue A5.42 is shown in red. The similar and distinct binding mode models of **1** and **tyramine** are outlined in green and blue dashed lines, respectively.

NIH-PA Author Manuscript

NIH-PA Author Manuscript

NIH-PA Author Manuscript

```
           N-Terminus                    TM1                          1.50
rTAAR1   MHLCHNSANISHTNSNWSR  DVRASLYSLISLIILTTLVGNLIVIISIS
mTAAR1   .....AIT....R..D...  E.Q......M.....A.............

           IL1            TM2          2.50                      EL1
rTAAR1   HFKQLHTPTN  WLLHSMAVVDFLLGCLVMPYSMVRTV  EHCWYFGE
mTAAR1   ..........  .......I........I..C......  .R......

           TM3         3.32                    3.50      IL2
rTAAR1   LFCKLHTSTDIMLSSASILHLAFISIDRYYAV  CDPLRYKAKIN
mTAAR1   IL..V.............F..........C..   ...........

           TM4            4.50      4.56          EL2
rTAAR1   LAAIFVMILISWSLPAVFAFGMIF  LELNLEGVEEQYHNQVFCLRGCFPFF
mTAAR1   IST.L....V.......Y......  .....K....L.RS..SD.G..S...

           TM5      5.42 5.43  5.46   5.50          IL3
rTAAR1   SKVSGVLAFMTSFYIPGSVMLFVYYRIY  FIAKGQARSINRANLQV
mTAAR1   ............................  ............T.V..

                         TM6                      6.48 6.50 6.52 6.54 6.55
rTAAR1   GLEGESRAPQS  KETKAAKTLGIMVGVFLLCWCPFFFCMVLDPFL
mTAAR1   ....K.Q....  ..................V......L.T......

           EL3          7.35     7.39     TM7      7.50
rTAAR1   GYVIPP  TLNDTLNWFGYLNSAFNPMVYAFFYPWFRRALKMVLF
mTAAR1   ......  S...A.Y........L....................L

           C-Terminus
rTAAR1   GKIFQKDSSRSKLFL
mTAAR1   ...............
```

Figure 5.

Sequence comparison of rat and mouse $TAAR_1$. Dots represent conserved residues. Amino and carboxy termini (N-terminus and C-terminus, respectively), intracellular loops (IL), extracellular loops (EL), and transmembrane regions (TM) are labeled. The most conserved residue in each TM region is labeled X.50 and residue 4.56 is highlighted in green.

NIH-PA Author Manuscript NIH-PA Author Manuscript NIH-PA Author Manuscript

Table 1

Agonist activity of **1**–**12** and **tyramine** on wild type rat and mouse $TAAR_1$

						rTAAR$_1$			mTAAR$_1$		
						EC$_{50}$ [a]	E$_{max}$ [b]	N [c]	EC$_{50}$ [a]	E$_{max}$ [b]	N [c]
Compd	**R$_1$**	**R$_2$**	**R$_3$**	**R$_4$**	**R$_5$**	**± SEM (nM)**	**± SEM (%)**		**± SEM (nM)**	**± SEM (%)**	
1 (T_1AM)	*p*-OH-Ph	I	H	H	-	33± 3	100± 0	5	314 ± 43	100 ± 0	5
2 (ET-13)	OPh	H	Ph	H	-	28 ± 2	103 ± 4	3	>10,000	35 ± 8	3
3 (ET-14)	H	OPh	Ph	H	-	19 ± 2	131 ± 7	3	>10,000	15 ± 4	3
5 (ET-36)	OPh	H	*p*- OH- Ph	H	-	6 ± 1	114 ± 9	4	>10,000	62 ± 6	3
6 (ET-64)	OPh	H	*p*- OH- Ph	CH_3	-	5 ± 1	127 ± 2	4	>10,000	42 ± 1	2
7 (ET-69)	*p*-OH-Ph	I	*p*- OH- Ph	H	-	4 ± 1	115 ± 2	6	>10,000	34 ± 5	3
8 (ET-71)	OH	H	Ph	H	-	78 ± 9	122 ± 16	3	>10,000	49	1
9 (ET-50)	OH	H	*p*- OH- Ph	H	-	115 ± 12	105 ± 5	3	>10,000	72	1
10 (PTA)	OPh	H	H	H	-	63 ± 7	93 ± 4	3	420 ± 66	85 ± 4	3
Tyramine	OH	H	H	H	-	65 ± 1	119 ± 7	3	271 ± 52	110 ± 2	3
4 (ET-21)	-	-	-	-	Ph	26 ± 1	113 ± 5	3	100 ± 22	104 ± 3	3
11 (ET-102)	-	-	-	-	*p*- OH-Ph	19 ± 3	96 ± 2	3	171 ± 13	98 ± 1	2
12 (1-NEA)	-	-	-	-	H	65 ± 6	115 ± 2	3	82 ± 17	112 ± 3	2

[a] EC_{50} is the half-maximal effective concentration of a compound.

[b] E_{max} is the maximum stimulation achieved at a concentration of 10 mM and was calculated by use of Prism software. EC_{50} and E_{max} values represent the average of N independent experiments in triplicate and were calculated by use of Prism software as escribed in the Methods section. E_{max} = 100 % is defined as the activity of **1** at 10 mM.

[c] N is the number of independent experiments in triplicate that were performed and used to calculate the EC_{50} and E_{max} values.

NIH-PA Author Manuscript
NIH-PA Author Manuscript
NIH-PA Author Manuscript

Table 2

Agonist activity of **1**, **3**–**5**, and **11** on $rTAAR_1$ TM 6 and/or 7 mutants

	$rTAAR_1$								
	M6.55T			**N7.39Y**			**M6.55T/N7.39Y**		
	EC_{50} [a]	**E_{max} [b]**	**N [c]**	**EC_{50} [a]**	**E_{max} [b]**	**N [c]**	**EC_{50} [a]**	**E_{max} [b]**	**N [c]**
Compd	**± SEM (nM)**	**± SEM (%)**		**± SEM (nM)**	**± SEM (%)**		**± SEM (nM)**	**± SEM (%)**	
1	129 ± 43	100 ±0	2	135	100	1	90	100	1
3	55 ± 20	119 ± 6	2	~10,000	85	1	>10,000	46	1
4	59 ± 0	117 ± 0	2	146	129	1	75	111	1
5	11 ± 1	117 ± 20	2	~1,000	126	1	~2,000	70	1
	$mTAAR_1$								
	T6.55M			Y7.39N			T6.55M/Y7.39N		
	EC_{50} [a]	E_{max} [b]	N [c]	EC_{50} [a]	E_{max} [b]	N [c]	EC_{50} [a]	E_{max} [b]	N [c]
Compd	± SEM (nM)	± SEM (%)		± SEM (nM)	± SEM (%)		± SEM (nM)	± SEM (%)	
1	1418 ± 592	100 ± 0	2	251 ± 43	100 ± 0	5	208 ± 60	100 ± 0	3
3	>10,000	20 ± 4	2	102 ± 21	95 ± 6	5	43 ± 5	110 ± 8	3
4	350 ± 101	96 ± 13	2	173 ± 41	93 ± 15	2	-	-	-
5	>10,000	45 ± 5	2	176 ± 32	91 ± 11	5	138 ± 24	101 ± 9	3
11	-	-	-	179 ± 21	92 ± 6	3	134 ± 43	101 ± 11	3

[a–c] See footnotes for Table 1. Compound structures are shown in Table 1.

NIH-PA Author Manuscript

NIH-PA Author Manuscript

NIH-PA Author Manuscript

Table 3

Agonist activity of **1**, **4**, **11**, and **tyramine** on $TAAR_1$ TM 4 or 5 mutants

a. $TAAR_1$ TM 5 mutants

	rTAAR$_1$								
	A5.42L			**A5.42I**			**A5.42T**		
	EC_{50} [a]	**E_{max} [b]**	**N [c]**	**EC_{50} [a]**	**E_{max} [b]**	**N [c]**	**EC_{50} [a]**	**E_{max} [b]**	**N [c]**
Compd	**± SEM (nM)**	**± SEM (%)**		**± SEM (nM)**	**± SEM (%)**		**± SEM (nM)**	**± SEM (%)**	
	58 ± 16	100 ± 0	3	108 ± 14	100 ± 0	3	88 ± 13	100 ± 0	4
Tyramine	~2,000	102 ± 18	3	>10,000	49 ± 7	3	>10,000	69 ± 5	4
11	32 ± 12	101 ± 8	3	29 ± 4	94 ± 2	3	25 ± 3	117 ± 13	4

b. $TAAR_1$ TM 4 mutants						
	rTAAR$_1$			**rTAAR$_1$**		
	A5.42L			**A5.42I**		
	EC_{50} [a]	**E_{max} [b]**	**N [c]**	**EC_{50} [a]**	**E_{max} [b]**	**N [c]**
Compd	± SEM (nM)	± SEM (%)		± SEM (nM)	± SEM (%)	
1	38 ± 11	100 ± 0	4	67 ± 17	100 ± 0	6
Tyramine	54 ± 11	108 ± 6	4	40 ± 13	118 ± 8	6
4	22 ± 5	101 ± 14	4	100 ± 16	123 ± 7	6
11	27 ± 15	101 ± 6	4	123 ± 41	105 ± 5	6

[a–c] See footnotes for Table 1. Compound structures are shown in Table 1.